

Structural and optical properties of europium doped Y_2O_3 nanoparticles prepared by self-propagation room temperature reaction method

Sanja Čulubrk, Vesna Lojpur, Željka Antić, and Miroslav D. Dramićanin*
*Vinča Institute of Nuclear Sciences, University of Belgrade,
PO Box 522, Belgrade, Serbia*

Received: December 24, 2013

Abstract

Europium-doped yttrium oxide nanoparticles with different doping concentrations were prepared by self-propagation room temperature reaction method. This simple synthesis method provides particles in the range of 12 nm to 50 nm, depending on the temperature of calcination. In all cases, the nanopowders showed intense red emission upon excitation with ultraviolet radiation. Structural and optical characterization showed that the nanoparticles obtained after calcination at 1100°C have smaller unit cell volume and microstrain and longer emission lifetimes compared to the nanoparticles obtained after calcination at 600°C and 800°C. The maximal emission intensity was found for the sample doped with 5 at% of Eu^{3+} .

Key words: Nanoparticles, phosphor, luminescence, Y_2O_3

1. Introduction

Rare-earth luminescent phosphors represent a significant class of materials since they find applications in biomedical multicolor imaging, scintillators, high-energy physics, for optical display and lighting [1], etc. Rare-earth sesquioxides, such as Y_2O_3 , are excellent host materials for doping with rare earth ions because they have excellent thermal and chemical stability, large thermal conductivity, large energy band gap, and transparency in the visible spectral range [2]. Among them yttrium oxide doped with trivalent europium (Eu^{3+}) is the most frequently used material to provide red light emission for modern optoelectronic devices [3, 4]. Rare-earth sesquioxides in the form of nanoparticles, nanorods, nanowires, nanotubes, as well as colloidal or bulk nanocrystals, are of interest not only for fundamental research, but also for many applications. For example, in the case of Eu^{3+} -doped yttrium oxide nanocrystals, the decrease of the particle size to several nanometers has been shown to have a large effect on the decay of the emitting excited states and the overall luminescence efficiency [5]. Also, sesquioxide nanopowders are excellent starting materials for preparation of transparent luminescence ceramics for the use in scintillation

*Corresponding author:

Email address: dramican@vinca.rs

detectors and lasers. Preparation of ceramics from nanopowders requires a lower temperature of sintering and the obtained products have higher fracture toughness and hardness [6].

Traditionally, sesquioxides are prepared using a solid state reaction method, starting with a mechanical mixing of precursor oxides, followed by a ball-milling and calcination. However, this method is time consuming, energetically inefficient, and yields powder with large particles. For preparation of submicron particles and nanoparticles of sesquioxides, various soft chemistry methods have been developed. These methods include hydrothermal synthesis [7], co-precipitation [8], sol-gel [9], combustion [10, 11], spray pyrolysis [12, 13], etc. Taking into account that the properties of materials at nanoscale strongly depend on their dimensions and morphologies, the search of novel methods for preparation of nanomaterials and study of their characteristics are of high interest of researchers. In this study we aimed to investigate potential of self-propagating room temperature (SPRT) method for the synthesis of europium doped yttrium oxide nanoparticles, as well as structure and luminescence properties of the particles obtained by this method.

2. Experimental

2.1. Synthesis of $\text{Y}_2\text{O}_3:\text{Eu}^{3+}$ nanoparticles

Nanocrystalline Y_2O_3 was synthesized via self-propagating room temperature method using yttrium nitrate hexahydrate (Alfa Aesar, 99.9 % purity), europium nitrate hexahydrate (Alfa Aesar, 99.9 % purity) and sodium hydroxide (Proanalytica, 99 %) as starting materials. A set of samples are prepared with different concentration of Eu^{3+} (1, 3, 5, 7 at%) dopant. The reaction was performed at room temperature after the mixture of reactants was mechanically activated by hand mixing in an alumina mortar for 5 min. After being exposed to air for a couple of hours, the mixture was washed in the centrifuge (3800 rpm, 10 min) five times with distilled water and two times with ethanol in order to eliminate NaNO_3 . Thereafter, the material was dried in a hot house for 12 h at 70°C . Sample with 5 at% of Eu^{3+} was thermally treated at 600°C , 800°C , 1100°C for 1 hour. The procedure is schematically shown in Figure 1.

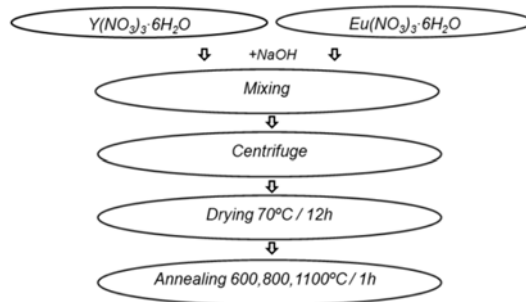


Figure 1. Schematic procedure of SPRT method.

2.2. Instruments and measurements

The infrared absorption spectra were recorded in the range of $4000 - 400 \text{ cm}^{-1}$ on a Nicolet spectrophotometer (Model 380 Thermo Nicolet Corporation, Madison USA), in

a reflection mode with a resolution of 4 cm^{-1} . The phase composition analysis of obtained powders was performed by X-ray powder diffraction (XRPD) analysis on a Rigaku Smart-Lab system operating with $\text{Cu K}_{\alpha 1,2}$ radiation at 40 mA and 30 kV. Data were taken in the 2θ range from 15° to 100° using continuous scan at a speed of $0.7^\circ/\text{s}$. Microstructure parameters were obtained using the Topas Academic software based on the Rietveld full profile refinement method. Photoluminescence measurements were performed at room temperature on a Fluorolog-3 Model FL3-221 spectrofluorometer system (Horiba Jobin-Yvon), utilizing the 450 W Xenon lamp as excitation source for emission measurements and a Xenon-Mercury pulsed lamp for lifetime measurements.

3. Results and discussion

3.1. Fourier transform infra-red (FTIR) measurements

Figure 2. shows the FTIR spectra of $\text{Y}_2\text{O}_3:5\text{ at}\% \text{Eu}^{3+}$ powder obtained after calcination at 1100°C for 1 hour. The FTIR shows that the obtained powders do not contain organic residues that may quench emission. A small amount of water molecules were detected (absorption of hydroxyl groups (OH^-) in the region of $3600 - 3000\text{ cm}^{-1}$), and these molecules are probably adsorbed on the surface of the particles.

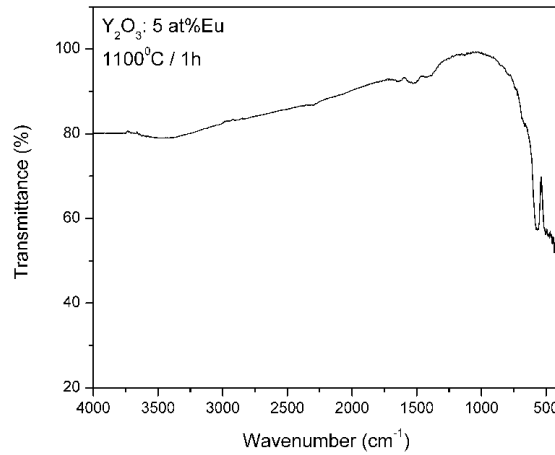


Figure 2. FTIR spectra of $\text{Y}_2\text{O}_3:5\text{ at}\% \text{Eu}$ powder calcined at 1100°C for 1 hour.

3.2. X-ray diffraction analysis (XRD)

The XRD patterns of Y_2O_3 doped with 5 at% of Eu^{3+} annealed at 600, 800, and 1100°C for 1 hour are presented in Fig. 3a. All samples have cubic crystal structure, space group Ia-3 and the appropriate peaks correspond to the pure Y_2O_3 phase (card no. PDF 00-025-1200). The reflections of samples thermally treated at higher temperatures have much narrower peaks, suggesting the increase in the particles crystallinity with rising of temperature. A detailed microstructural analysis was performed by the Rietveld refinement (Table 1 and Fig. 3b). The crystallite size is increasing from 12 nm for the sample calcined at 600°C to 50 nm for the sample calcined at 1100°C . At the same time, cell parameter decreased as a consequence of better crystallization of samples and incorporation

of dopant ion in the structure. Also, with rising of temperature, substantial reduction of microstrain was observed.

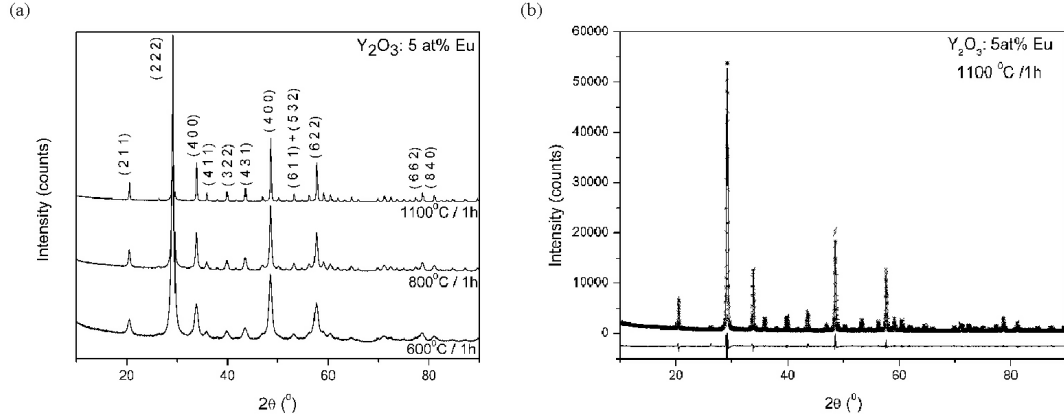


Figure 3. (a) XRPD patterns of $\text{Y}_2\text{O}_3:5 \text{ at\% Eu}^{3+}$, thermally treated at 600, 800 and 1100°C for 1h (b) Example of structural refinement for sample calcined at 1100°C for 1h. Final Rietveld plot: the observed (crosses), calculated (solid line) and difference XRD patterns.

Table 1. Selected structural parameters obtained by XRD measurements and after Rietveld refinements for $\text{Y}_2\text{O}_3:5 \text{ at\% Eu}^{3+}$ nanopowders.

	600°C/1 h	800°C/1 h	1100°C/1 h
Crystallite size (nm)	12.545(4)	22.732(7)	50.620(0)
Cell parameter (Å)	10.6105(1)	10.603198)	10.6000
Microstrain (%)	0.24889	0.08761	0.0001
*Y ₁ :O bond length (Å)	2.19739	2.22206	2.21872
	2.31724	2.28909	2.28169
	2.35410	2.35144	2.34900
	2.28264	2.27915	2.29315
*Y ₂ :O bond length (Å)			
Y ₁ (Y ³⁺ , Eu ³⁺)	-0.02936	-0.03114	-0.03234
X			
O ²⁻			
x	0.93033	0.39105	0.39247
y	0.15432	0.15349	0.15336
z	0.38203	0.38036	0.38099
R _{wp}	3.8573(6)	3.9211(5)	6.2135(2)
R _p	3.0124(0)	3.0012(4)	4.7096(0)
GOF	1.381(1)	1.392(1)	2.176(8)

*Y₁ corresponds to C₂ site ; *Y₂ corresponds to S₆ site in cubic crystal unit cell

3.3. Photoluminescent spectroscopy

The luminescence emission spectra of all samples clearly show five characteristic peaks centered around 580, 593, 610, 650, 708 nm that correspond to $^5\text{D}_0 \rightarrow ^7\text{F}_0$, $^7\text{F}_1$, $^7\text{F}_2$, $^7\text{F}_3$,

7F_4 spin forbidden f-f electron transitions, respectively. (see Fig. 4). The $^5D_0 \rightarrow ^7F_1$ transition is the parity-allowed magnetic dipole transition, and its intensity does not vary with the host. On the contrary, $^5D_0 \rightarrow ^7F_2$ electric dipole transition is highly sensitive to the local environment around Eu^{3+} , and its intensity depends on the symmetry of the crystal field around the europium ion. For europium ions residing in the centrosymmetric S_6 site only weak magnetic dipole transitions are possible, therefore only a low-intensity luminescence peak from S_6 site may be observed, while all other luminescence comes from europium ions residing in the C_2 site. The photoluminescence spectra for $Y_2O_3:Eu^{3+}$ -doped with different concentrations (1, 3, 5 and 7 at%), and the spectra for $Y_2O_3:5\text{ at\% } Eu^{3+}$ sample calcined at several temperatures (600°C , 800°C , and 1100°C for 1 hour) are shown in Figs. 4 and 5. respectively.

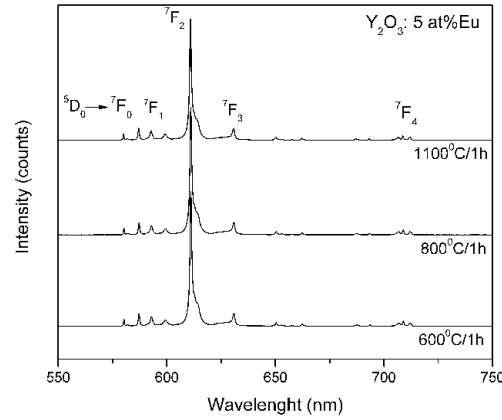


Figure 4. Photoluminescence emission spectra of Y_2O_3 doped with different concentrations of Eu^{3+} (1, 3, 5 and 7 at%).

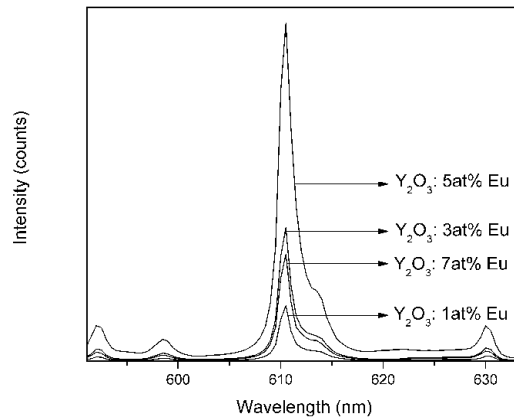


Figure 5. Photoluminescence emission spectra of $Y_2O_3:5\text{ at\% } Eu^{3+}$ samples calcined for 1 hour at 600°C , 800°C , and 1100°C .

The emission intensity increases with the concentration of europium dopant, Figure 4, with a maximal intensity reached at a concentration of 5 at%. For higher concentrations the emission intensity is lower due to the concentration quenching effect. The effect of

annealing temperature on the photoluminescence spectra of $\text{Y}_2\text{O}_3:5\text{ at}\% \text{Eu}^{3+}$ samples are presented in Fig. 5. The ratio of the integrated emission intensity (asymmetry ratio) of the $^5\text{D}_0 \rightarrow ^7\text{F}_2$ and $^5\text{D}_0 \rightarrow ^7\text{F}_1$ transitions can be considered as indicative of the symmetry of the coordination environment around the Eu^{3+} ion. The values of this ratio are 5.24 for the sample annealed at 600°C , 5.22 for the one annealed at 800°C , and 4.88 for the nanopowders annealed at 1100°C . This result is in agreement with the results obtained for the microstrain by structural analysis (Table 1). Calcination at higher temperatures produces powder with better structural ordering, and, in that case, the value of the microstrain is minimal. In that case the first coordination sphere around Eu^{3+} ions has lower distortions, and consequently, the photoluminescence emission spectrum shows a lower asymmetry ratio coefficient. The emission decays are measured at 611 nm, and the values of $^5\text{D}_0$ excited state lifetimes are presented in Table 2. The slightly larger values of lifetimes are observed for the samples annealed at higher temperatures. This is a consequence of a more efficient removal of water molecules from the surface of nanoparticles by annealing at larger temperatures. Also, annealing at larger temperature induces shortening of the $\text{Eu}^{3+} - \text{O}_2^-$ distances (see the values of the unit cell volumes in Table 1) which results in a slight increase in the lifetime values. The Eu^{3+} concentration effect on the excited state lifetimes follow the same trend as in the case of the emission intensities. The greatest value is found for the sample doped with 5 at% of Eu^{3+} .

Table 2. Lifetime values for $\text{Y}_2\text{O}_3: 5\text{ at}\% \text{Eu}^{3+}$ sample and for $\text{Y}_2\text{O}_3:\text{Eu}^{3+}$ - doped with different concentrations (1, 3, 5 and 7 at%) obtained after calcination.

	600°C/1 h	800°C/1 h	1100°C/1 h	
$\text{Y}_2\text{O}_3: 5\text{ at}\% \text{Eu}$	1.69 ms	1.71 ms	1.76 ms	
	1 at% Eu	3 at% Eu	5 at% Eu	7 at% Eu
$\text{Y}_2\text{O}_3: x\text{ at}\% \text{Eu}$	1.11 ms	1.69 ms	1.84 ms	1.55 ms
1100°C/4 h				

4. Conclusion

The self-propagating room temperature reaction method is capable to produce Eu^{3+} doped Y_2O_3 nanoparticles that emit red light upon excitation in the ultraviolet spectral range. This method is simple, energetically efficient, and utilizes only metal nitrates and NaOH for nanoparticle preparation. At different temperatures of annealing yield the powders with crystallite size from 12 nm to 50 nm. Also, with high annealing temperatures particles with a smaller unit cell volume, lower microstrain values, and larger emission lifetime values are produced. Intense red emission is emitted from the nanoparticles after excitation with ultraviolet radiation, with the strongest emission peak at 611 nm due to the trivalent europium ions. The maximal emission intensity is achieved with 5 at% of Eu^{3+} .

Acknowledgments

This work is supported by the Ministry of Education, Science and Technological Development of the Republic of Serbia (Grant numbers 45020 and 17035).

References

- [1] R. M. Krsmanovic, Ž. Antic, M. G. Nikolic, M. Mitric and M. D. Dramicanin, *Ceram. Int.* **37**, 525 (2011).
- [2] R. M. Krsmanovic, Ž. Antic, B. Bártoová and M. D. Dramićanin, *J. Alloy. Compd* **505**, 224 (2010).
- [3] R. Schmechel, M. Kennedy, H. von Seggem, H. Winkler, M. Kolbe, R. Fisher, L. Xiaomao, A. Benker, M. Winterer and H. Hahn, *J. Appl. Phys.* **89**, 1679 (2001).
- [4] M. Z. Su and W. Yhao, Rare earths ions in advanced X-ray imaging materials, in: L. Guokui, J. Bernard (Eds.), *Spectroscopic Properties of Rare Earths in Optical Materials*, p. 521 (Springer-Verlag, Berlin/Heidelberg, 2005).
- [5] F. Vetrone, John-Christopher Boyer, J. A Capobianco, A. Speghini and M. Bettinelli, *Nanotechnology* **15**, 75 (2004).
- [6] R. M. Krsmanović, Ž. Antić, B. Bártoová, M. G. Brik and M. D. Dramićanin, *Ceram. Int.* **38**, (2012) 1303.
- [7] M. K. Devaraju, S. Yin and T.Sato, *Eur. J. Inorg. Chem* **29-30**, 4441 (2009).
- [8] J. Li, Y. Zhang, G. Hong and Y. Yu, *J. Rare Earths* **26**, 450 (2008).
- [9] Q. Yanmin and G.Hai, *J. Rare Earths* **27**, 406 (2009).
- [10] D. L. Phan, M. H. Phan, N. Vu, T. K. Anh and S.C. Yu, *Phys. Status Solidi* **201**, 2170 (2004).
- [11] Ž. Antić, R. Krsmanović, M. Wojtowicz, E. Zych, B. Bártoová and M. D. Dramićanin, *Opt. Mater.* **32**, 1612 (2010).
- [12] Ž. Antić, R. Krsmanović, V. Đorđević, T. Dramićanin and M. D. Dramićanin, *Acta Physica Polonica A* **116**, 622 (2010).
- [13] K. Marinkovic, L. Mancic, L. S. Gomez, M. E. Rabanal, M. Dramicanin and O. Milosevic, *Opt. Mater.* **32**, 1606 (2010).